Journal of the European Ceramic Society 23 (2003) 537–545

www.elsevier.com/locate/jeurceramsoc

# Hot-pressed silicon nitride ceramics with $Lu_2O_3$ additives: elastic moduli and fracture toughness

Shuqi Guo*, Naoto Hirosaki, Yoshinobu Yamamoto, Toshiyuki Nishimura, Mamoru Mitomo

*Advanced Materials Laboratory, National Institute for Materials Science, 1-1 Namiki, Tsukuba, Ibaraki 305-0044, Japan*

Received 26 April 2001; received in revised form 20 March 2002; accepted 1 April 2002

**Abstract**

The elastic moduli and fracture toughness of hot-pressed $Si_3N_4$ ceramics, using 1.68, 3.33, 6.52 and 12.51 wt.% of $Lu_2O_3$ additives, were studied by means of ultrasonic measurements and Vickers indentation crack size measurements, respectively. The elastic moduli were found to increase with the amount of $Lu_2O_3$ additive for silicon nitride which was not completely densified. However, the elastic moduli remained nearly constant independent on the amount of additive for completely dense silicon nitride. The elastic moduli of completely dense silicon nitride should reach the following average values: shear modulus $G=132$ GPa, Young's modulus $E=338$ GPa, bulk modulus $B=255$ GPa and Poisson's ratio $\nu=0.28$. On the other hand, the fracture toughness showed a clear dependence of additive amount for both incompletely and completely dense silicon nitride ceramics. The fracture toughness increased with additive amount over the range 1.68 to 12.51 wt.% $Lu_2O_3$. The improvement in the fracture toughness with the amount of additive was mainly attributed to elongated grain growth during the sintering process. 

*Keywords:* Elastic moduli; Fracture toughness; Hot-pressing; $Lu_2O_3$ additive; $Si_3N_4$

## 1. Introduction

Silicon nitride ($Si_3N_4$) ceramics have become an important class of materials for structural applications; because they have excellent high-temperature strength, good resistance to oxidation, high creep resistance, low coefficient of thermal expansion, good resistance to thermal shock and chemical attack.[1–9] However, it is difficult to sinter pure silicon nitride ceramics due to the low self-diffusivity of this type of covalent material.[10] To improve sinterability oxides such as $Y_2O_3$, $Al_2O_3$, MgO, $Sc_2O_3$, $ZrO_2$ or $Yb_2O_3$ are added to pure silicon nitride, providing the formation of a intergranular liquid phase which aids in the densification of the silicon nitride during the sintering process.[1–9] The mechanical properties, such as elastic moduli, strength, fracture toughness, creep and resistance to oxidation, of the $Si_3N_4$ ceramics sintered using these additives have been well studied.[1–9] These studies demonstrate that the degradation seen in the mechanical properties of $Si_3N_4$ at elevated temperatures depends strongly on the characteristics of the grain boundary phase, which is determined by the sintering process, additive type and amount. In general, $Si_3N_4$ containing a secondary grain boundary phase which has a high melting point and is extensively crystallized, has a higher strength at elevated temperature than that of a material containing an amorphous phase with lower viscosity,[1–4] while larger and elongated grains result in increased fracture toughness by mainly crack bridging.[5,6] The well-known $Si_3N_4$ material produced using the $Yb_2O_3$ additive has been reported to have high and stable mechanical properties up to 1400 °C due to the crystalline $Yb_4Si_2O_7N_2$ grain boundary phase.[3,4] However, above 1400 °C it is also found that there is a sharp degradation of these properties. It is clear that higher temperature resistance is desirable and thus further development of $Si_3N_4$ materials is required.

A new type of $Si_3N_4$, using $Lu_2O_3$ as a sintering additive developed recently has unique high-temperature strength and oxidation resistance[11–13] up to 1500 °C.

* Corresponding author. Fax: +81-298-51-3613.
*E-mail address:* guo.shuqi@nims.go.jp (S. Guo).

0955-2219/02/$ - see front matter 
PII: S0955-2219(02)00091-2

Few studies have reported the strength and oxidation properties of these ceramics at elevated temperatures.[11–13] Furthermore, the properties such as the elastic moduli and fracture toughness have not been reported. The present paper is focused on the experimental determination of the elastic moduli and fracture toughness of hot-pressed $Si_3N_4$ ceramics with $Lu_2O_3$ additives, using ultrasonic testing and the Vickers indentation technique, respectively. Moreover, the effect of the amount of additive on these properties is also discussed.

## 2. Experimental procedure

### 2.1. Materials

The starting powders used in the present study were an α-rich $Si_3N_4$ (SN-E10, UBE Industries, Tokyo, Japan) and $Lu_2O_3$ (99.9% purity, Shinetsu Chemical Co., Ltd., Tokyo, Japan). The $Lu_2O_3$ powder was added to the $Si_3N_4$, and the powder batches were mixed in ethanol for 2 h using a $Si_3N_4$ ball mill, and then dried in a rotation evaporator. The mixed powder was then preformed into a rectangle, 80 × 45 × 13 mm, in a metal die using cold pressing at 20 MPa. The preforms of the mixture of $Si_3N_4$ were placed in a carbon die coated with BN powder, and a thin carbon plate was added between these preforms to separate them. Subsequently, these preforms were sintered for 1 h at 1950 °C with a heating rate of 20 °C/min to 1200 °C and then 10 °C/min to 1950 °C under a pressure of 20 MPa in ~1 MPa nitrogen gas environment using a gas-sintering furnace (FVPHR-R-10, FRET-40, Fuji Electric Co., Ltd., Tokyo, Japan). $Si_3N_4$ ceramics with 1.68, 3.33, 6.52 and 12.51 wt.% $Lu_2O_3$ additive amounts were fabricated, and their density, $\rho$, was evaluated by the Archimedes method.

The hot-pressed $Si_3N_4$ materials were cut, and the resulting surface was polished with a diamond paste up to 0.25 μm. The surface of the polished specimens was then etched with a $CF_4$ plasma containing 7.8% $O_2$. The morphology of the $Si_3N_4$ microstructure was characterized by scanning electron microscope (SEM). These micrographs were then quantitatively analyzed using an image processing system (LUZEX III, Nireko Co., Ltd., Tokyo, Japan). Minimums of 300 grains in each material were analyzed. The crystalline phase compositions were identified by X-ray diffractometry (XRD).

### 2.2. Elastic moduli measurement

For the elastic moduli measurements, the hot-pressed $Si_3N_4$ plates were cut into a rectangle shape specimen with dimensions of ~40 × 4 × 3 mm, and each specimen was ground and polished to obtain parallel opposite faces of better than 3 μm. Before the measurement, the specimen thickness, $h$, was measured using a micrometer with an accuracy of 1 μm. The elastic moduli of the specimen were determined using ultrasonic equipment (EXPLORER-9000, Matec Instruments, MA, USA) with a fundamental frequency of 15 MHz. The Young's modulus, $E$, shear modulus, $G$, bulk modulus, $B$, and Poisson's ratio, $\nu$, are given by[14,15]

$$E = \rho V_t^2 \left( \frac{3V_l^2 - 4V_t^2}{V_l^2 - V_t^2} \right), \tag{1a}$$

$$G = \rho V_t^2, \tag{1b}$$

$$B = \frac{EG}{3(3G - E)}, \tag{1c}$$

$$\nu = \frac{E}{2G} - 1, \tag{1d}$$

where $\rho$ is the density, $V_l$ and $V_t$ are the longitudinal and transverse soundwave velocities, respectively, and the $V_l$ and $V_t$ were determined by

$$V_l = \frac{2h}{\Delta t_l}, \tag{2a}$$

$$V_t = \frac{2h}{\Delta t_t}, \tag{2b}$$

where $\Delta t_l$ and $\Delta t_t$ are the elapsed times between the pulse and the echo of the longitudinal and transverse waves, respectively. The accuracy of the soundwave velocity measurement was found to be better than 1%.

### 2.3. Fracture toughness measurement

The fracture toughness, $K_{IC}$, of the hot-pressed $Si_3N_4$ was determined using an indentation crack size measurement. The indentation tests were performed on the polished surface of the specimens by loading with a Vickers indenter (AVK-A, Akashi, Co., Ltd., Yokohama, Japan) for 20 s in air at room temperature. The corresponding diagonal of the indentation and crack sizes were measured using an optical microscope attached to the indenter. Three indentation loads of 98, 196 and 294 N were used, and five indents were made at each indentation load.

The fracture toughness, $K_{IC}$, was calculated using the following relation,[16]

$$K_{IC} = 0.016 \left( \frac{E}{H_v} \right)^{1/2} \frac{P}{c^{3/2}}, \tag{3}$$

where $E$ is the Young's modulus (GPa), $H_v$ is the hardness (GPa), $P$ is the indentation load (N) and $c$ is the

crack length (μm). The hardness, $H_v$, was calculated from,

$$H_v = 1854.4\frac{P}{d^2}, \quad (4)$$

where $d$ is the diagonal of the indentation (μm).

## 3. Results and discussion

### 3.1. Density, microstructure and crystalline phases

Fig. 1 represents several plots of average density and relative density of the hot-pressed $Si_3N_4$ ceramics against amount of $Lu_2O_3$ additive. The average density was found to be, $\rho = 3181$ kg/m$^3$ for 1.68 wt.%, $\rho = 3274$ kg/m$^3$ for 3.33 wt.%, $\rho = 3350$ kg/m$^3$ for 6.52 wt.%, and $\rho = 3495$ kg/m$^3$ for 12.51 wt.%. The measured density, $\rho$, increases with the increase in amount of $Lu_2O_3$ additive, and the increase rate correlates to amount of $Lu_2O_3$ additive; the increase rate at lower amount of $Lu_2O_3$ additive ($\leqslant 3.33$ wt.%) is larger than one at higher amount of $Lu_2O_3$ additive ($> 3.33$ wt.%). The increase in the density of $Si_3N_4$ with amount of $Lu_2O_3$ additive should be attributed to the formation of an intergranular amorphous phase.[17] The relative density is defined as $\rho/\rho_t$ where $\rho_t$ is the theoretical density of the mixture of $Si_3N_4$ and is calculated using the role of mixture. The theoretical density of pure $Si_3N_4$ was taken as 3190 kg/m$^3$ and that of pure $Lu_2O_3$ as 9410 kg/m$^3$. The relative density reveals a different dependence of $Lu_2O_3$ amount against the density. The relative density increases with the amount of additive used from 1.68 to 3.33 wt.%. For amounts higher than 3.33 wt.% it is independent on amount of $Lu_2O_3$ additive and approximately equal to unit, this means that at least 3.33 wt.% $Lu_2O_3$ is needed to obtain completely dense $Si_3N_4$ from the sintering process.

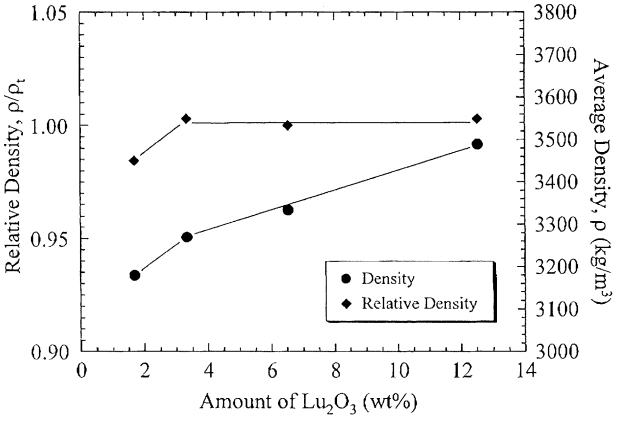


Fig. 1. Relative density and average density of the hot-pressed $Si_3N_4$ ceramics against amount of $Lu_2O_3$ additives.

Fig. 2 shows SEM micrographs of microstructures for the hot-pressed $Si_3N_4$ ceramics with $Lu_2O_3$ additives. The histograms of grain-section diameter are also shown. In these micrographs, the β-$Si_3N_4$ grains are seen in dark contrast, while the grain boundary phase appears in light contrast. The material microstructure can be described with respect to the additive content as follows: for 1.68 wt.% $Lu_2O_3$-containing $Si_3N_4$ material there are a few elongated grains in a fine grains microstructure [Fig. 2(a)]; with further increase in amount of additive, the grains become coarser [Fig. 2(b)], especially the amount of the elongated grains significantly increases as the amount of additive is equal to or greater than 6.52 wt.% [Fig. 2(c) and (d)]. In addition, a broad grain diameter size distribution is observed for the hot-pressed $Si_3N_4$ ceramics with $Lu_2O_3$ additives [Fig. 2(e)–(g)], with exception of the 12.51 wt.% composition ceramic exhibits a bimodal grain diameter size distribution although this bimodal distribution is not very noticeable [Fig. 2(h)]. A change of the grain-section diameter with amount of additive is shown in Fig. 3. This shows that an increase of the additive accelerates grain growth and coarsening. On the other hand, a thin grain boundary phase, with net-like shape, is observed in the hot-pressed $Si_3N_4$ ceramics with 1.68 and 3.33 wt.% $Lu_2O_3$ additives [Fig. 2(a) and (b)]. However, the grain boundary phase becomes thicker and the net-like structure becomes small and/or partially disappearance as the amount of additive is greater 3.33 wt.% (Fig. 2(c) and (d). X-ray diffraction patterns show that the grain boundary phase consists of crystalline $Lu_4Si_2O_7N_2$ phase for all compositions $Si_3N_4$ materials (Table 1), trace amount of crystalline $Lu_2SiO_5$ phase is also present for the 12.51 wt.% $Lu_2O_3$-containing $Si_3N_4$, however. Electron microscopy study[18] confirmed very recently a completely crystalline $Lu_4Si_2O_7N_2$ secondary phase for the hot-pressed $Si_3N_4$ with a lower amount of $Lu_2O_3$ additive, e.g. 3.33 wt.% $Lu_2O_3$ composition ceramic, and for the $Si_3N_4$ with a higher amount of $Lu_2O_3$ additive approximately half of the triple-grains junctions pockets were devitrification, e.g. 12.51 wt.% $Lu_2O_3$ composition case.

### 3.2. Elastic moduli

Fig. 4 shows the measured elastic moduli of the hot-pressed $Si_3N_4$ ceramics with $Lu_2O_3$ additives. The measured average shear modulus, $G$, Young's modulus, $E$, bulk modulus, $B$, and Poisson's ratio, $\nu$, are given as follows: $G = 124.8$, $E = 319.7$ and $B = 243.0$ GPa and $\nu = 0.281$ for 1.68 wt.%, $G = 132.4$, $E = 338.0$ and $B = 251.3$ GPa and $\nu = 0.276$ for 3.33 wt.%, $G = 132.2$, $E = 338.1$ and $B = 254.5$ GPa and $\nu = 0.279$ for 6.52 wt.%, and $G = 132.6$, $E = 340.0$ and $B = 260.0$ GPa and $\nu = 0.282$ for 12.51 wt.%. The elastic moduli obtained for completely dense silicon nitride are slightly higher

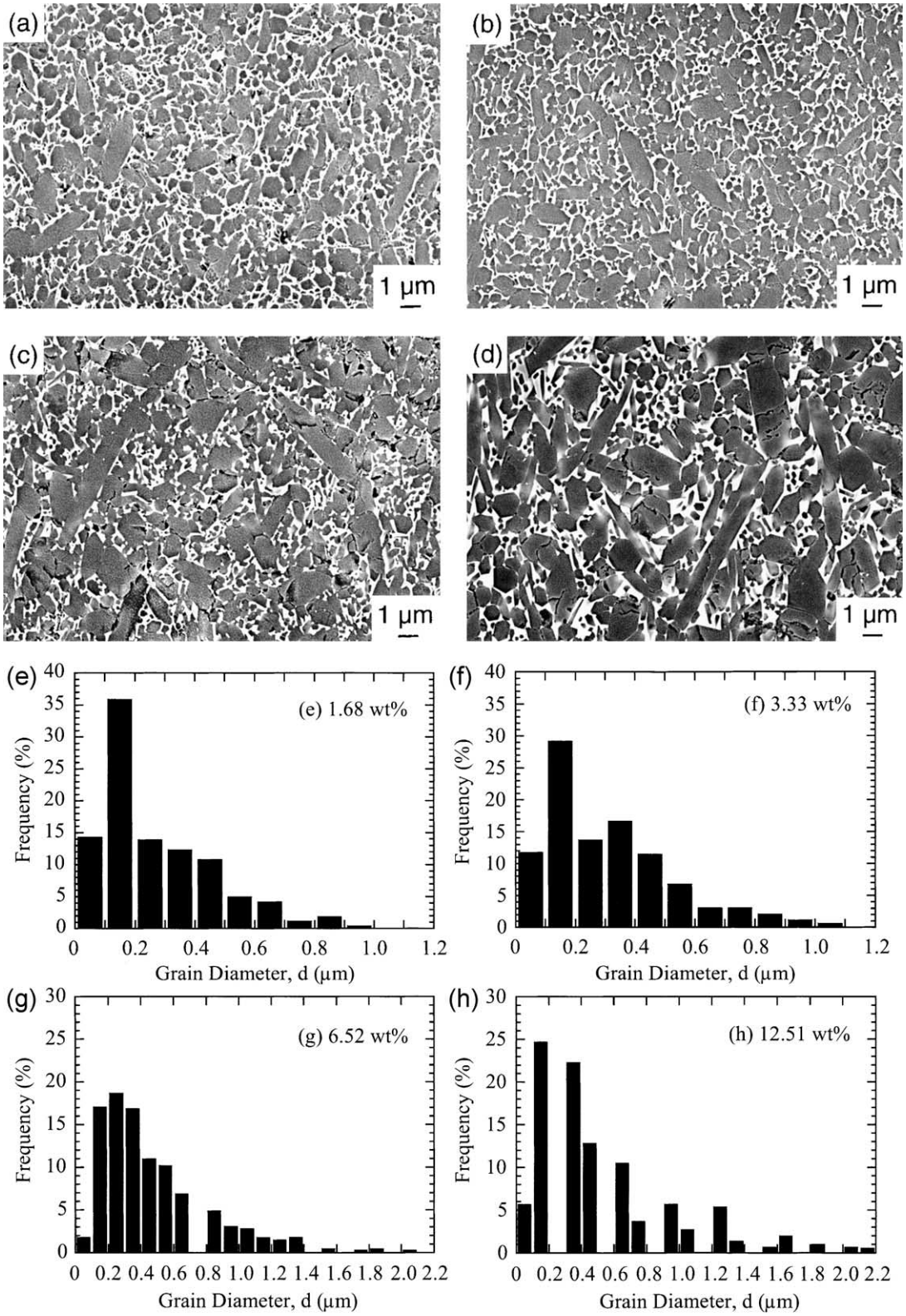


Fig. 2. SEM micrographs of microstructures of the hot-pressed $Si_3N_4$ ceramics with $Lu_2O_3$ additives of (a) 1.68, (b) 3.33, (c) 6.52 and (d) 12.51 wt.%. The corresponding histograms of the grain-section diameter are given in (e), (f), (g) and (h), respectively.

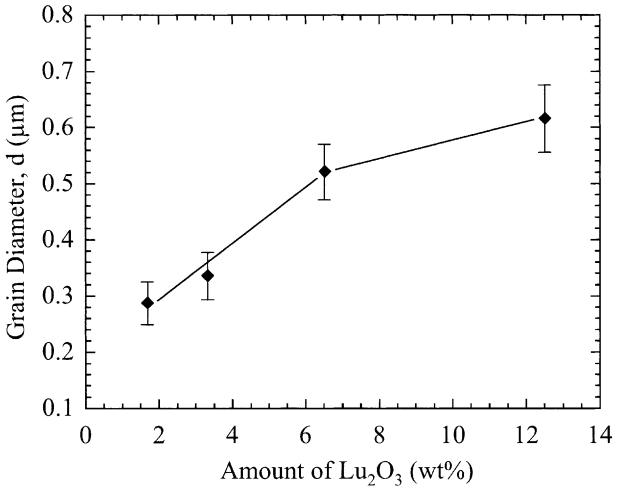


Fig. 3. Average grain diameter of the hot-pressed $Si_3N_4$ ceramics versus amount of $Lu_2O_3$ additives.

than those of $Si_3N_4$ with other additives, reported elsewhere.[3,5,17] In addition, the shear modulus, Young's modulus and bulk modulus are found to increase with the amount of $Lu_2O_3$ additive for the $Si_3N_4$ which is not completely densified ($\rho/\rho_t = 0.985$ for 1.68 wt.% $Lu_2O_3$ composition ceramic). However, both the shear modulus and Young's modulus remain nearly constant and the bulk modulus increases slightly with a further increase in the amount of additive for the completely dense $Si_3N_4$ ($\rho/\rho_t = 1.0$ for $\geqslant 3.33$ wt.% $Lu_2O_3$ composition ceramics). This finding indicated that the pore volume is a main factor that affects the elastic moduli of the $Si_3N_4$ materials. The bulk modulus increases slightly with increase in the amount of additive; this is probably attributed to an increase in the amount of the grain boundary phases, and the change of their compositions and residual stresses caused by crystallization of these phases during the sintering process. This is the case, because the bulk modulus has a greater sensitive in a change of these factors than both the shear and Young's moduli.[15] However, Poisson's ratio is nearly constant for either incompletely or completely dense $Si_3N_4$, as well as is independent on the amount of additive in the range of the present test, showing that this parameter is insensitive to the pore fraction for the $Si_3N_4$ specimen sintered with a high-density (relative density $>98\%$).

Table 1
Crystalline phases present in the hot-pressed $Si_3N_4$ ceramics with $Lu_2O_3$ additives

| Amount of $Lu_2O_3$ (wt.%) | Primary phase | Secondary phase | Minor phase |
|---|---|---|---|
| 1.68 | β-$Si_3N_4$ | $Lu_4Si_2O_7N_2$ | |
| 3.33 | β-$Si_3N_4$ | $Lu_4Si_2O_7N_2$ | |
| 6.52 | β-$Si_3N_4$ | $Lu_4Si_2O_7N_2$ | |
| 12.51 | β-$Si_3N_4$ | $Lu_4Si_2O_7N_2$ | $Lu_2SiO_5$ |

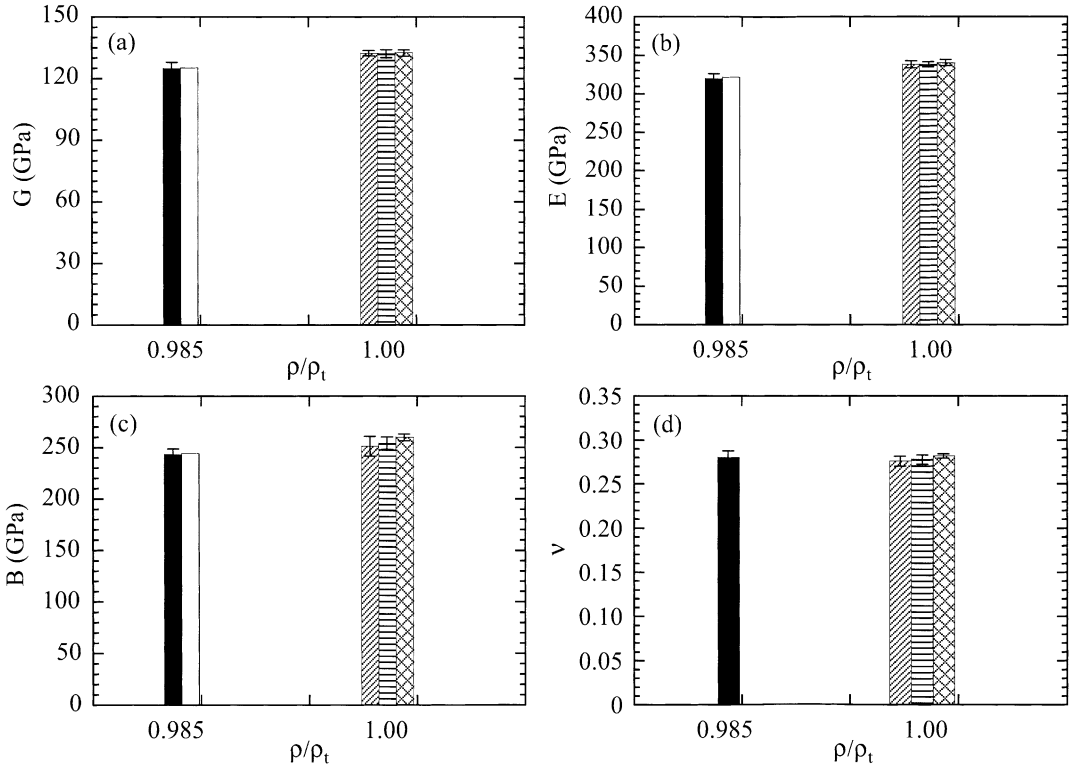


Fig. 4. Elastic moduli of the hot-pressed $Si_3N_4$ ceramics with $Lu_2O_3$ additives against relative density, (a) shear modulus, (b) Young's modulus, (c) bulk modulus and (d) Poisson's ratio ( ■ 1.68 wt.%, ▨ 3.33 wt.%, ▤ 6.52 wt.%, ▩ 12.51 wt.%, □ Predicted for 1.68 wt.%).

Assuming that the effect of pore structure on elastic moduli is neglected, the elastic moduli can be given as[14]

$$M = M_0(1 - \eta V_p) \quad (5)$$

where $M$ and $M_0$ are the elastic moduli ($G$, $E$ and $B$) at volume fraction porosity, $V_p$ ($= 1 - \rho/\rho_t$), and zero, respectively, and $\eta$ is a constant for each elastic modulus. The calculated maximum values of the completely dense $Si_3N_4$ are defined as $G_0$, $E_0$ and $B_0$, and $G_0 = 132.6$, $E_0 = 340.0$ and $B_0 = 260.0$ GPa. Assuming that $\eta$ is independent of additive kinds, it is 3.62 for $G$, 3.47 for $E$ and 3.95 for $B$ according to reported data in Ref. [17] for the present $Si_3N_4$ materials. The predicted elastic moduli for the hot-pressed 1.68 wt.% $Lu_2O_3$-containing $Si_3N_4$ ceramic are given in Fig. 4 by the dotted column. This is consistent with the measured elastic moduli values for the $Si_3N_4$ with 1.68 wt.% $Lu_2O_3$ that contains 1.5% porosity.

Fig. 5 shows a change of the measured soundwave velocity with amount of additive for the hot-pressed $Si_3N_4$ ceramics. The average soundwave velocities are as follows: $V_l = 11345$ and $V_t = 6264$ m/s for 1.68 wt.%, $V_l = 11431$ and $V_t = 6359$ m/s for 3.33 wt.%, $V_l = 11339$ and $V_t = 6282$ m/s for 6.52 wt.%, $V_l = 11179$ and $V_t = 6160$ m/s for 12.51 wt.%. Differing with the elastic moduli, the soundwave velocity depends on amount of additive in $Si_3N_4$, although this dependence is weak. Both the longitudinal and transverse soundwave velocities increase initially as the amount of additive begins to increase, the soundwave velocities achieve a maximum value at 3.33 wt.% $Lu_2O_3$, and then they decrease slowly with the continuous increase in the amount of additive. This seems to attribute to an increase in the amount of the grain boundary phase and its composition change, because the thicker intergraular phase layer and complex phases between grains hinder the transmission of soundwaves.

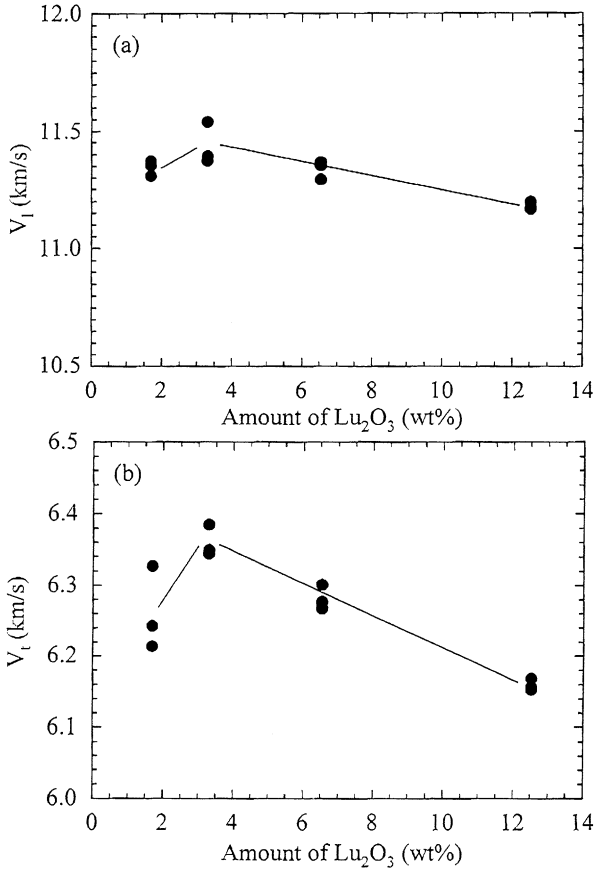


Fig. 5. Change of measured longitudinal soundwave velocity (a) and transverse soundwave velocity (b) with amount of $Lu_2O_3$ additives for the hot-pressed $Si_3N_4$ ceramics.

The measured density, soundwave velocity and elastic moduli of the hot-pressed $Si_3N_4$ ceramics with various amounts of the $Lu_2O_3$ additive are summarized in Table 2 .

### 3.3. Fracture toughening

The hardness and fracture toughness of the hot-pressed $Si_3N_4$ ceramics with $Lu_2O_3$ additives determined by indentation crack size measurements are plotted against the amount of additive in Fig. 6 . The hardness of the $Si_3N_4$, $H_v$, shows a slight increase from 1.68 wt.% to 3.33 wt.% of $Lu_2O_3$, then a slow decrease is observed as the amount of additive is increased further. The hardness for 12.51 wt.% $Lu_2O_3$-containing $Si_3N_4$ ceramic is nearly equal to that of 1.68 $Lu_2O_3$-containing $Si_3N_4$ ceramic, showing a slight dependence on amount of additive. Conversely, the fracture toughness, $K_{IC}$, shows a clear dependence of additive amount and increases with an increase in amount of additive; the rate of increase from 1.68 to 6.52 wt.% of $Lu_2O_3$ is greater than that from 6.52 wt.% to 12.51 wt.% of $Lu_2O_3$. Note that

Table 2
Measured densities, soundwave velocities and elastic moduli of the hot-pressed $Si_3N_4$ ceramics with $Lu_2O_3$ additives

| Amount of $Lu_2O_3$ (wt.%) | Density $\rho$(kg/m$^3$) | Soundwave velocity (m/s) | | Elastic moduli | | | |
|---|---|---|---|---|---|---|---|
| | | $V_l$ | $V_t$ | $G$ (GPa) | $E$ (GPa) | $B$ (GPa) | $v$ |
| 1.68 | 3182 | 11,309 | 6243 | 124.1 | 317.8 | 241.6 | 0.281 |
| | 3180 | 11,354 | 6334 | 127.6 | 325.1 | 239.8 | 0.274 |
| | 3180 | 11,373 | 6214 | 122.8 | 316.1 | 247.6 | 0.287 |
| 3.33 | 3261 | 11,542 | 6385 | 133.0 | 340.3 | 257.2 | 0.280 |
| | 3282 | 11,374 | 6345 | 132.2 | 336.8 | 248.4 | 0.274 |
| | 3279 | 11,377 | 6347 | 132.1 | 336.6 | 248.3 | 0.274 |
| 6.52 | 3353 | 11,294 | 6301 | 133.1 | 339.2 | 250.2 | 0.274 |
| | 3352 | 11,354 | 6268 | 131.7 | 337.4 | 256.5 | 0.281 |
| | 3345 | 11,369 | 6277 | 131.8 | 337.6 | 256.7 | 0.281 |
| 12.51 | 3491 | 11,166 | 6153 | 132.2 | 338.9 | 259.1 | 0.282 |
| | 3492 | 11,174 | 6157 | 132.4 | 339.4 | 259.5 | 0.282 |
| | 3503 | 11,196 | 6169 | 133.3 | 341.8 | 261.3 | 0.282 |

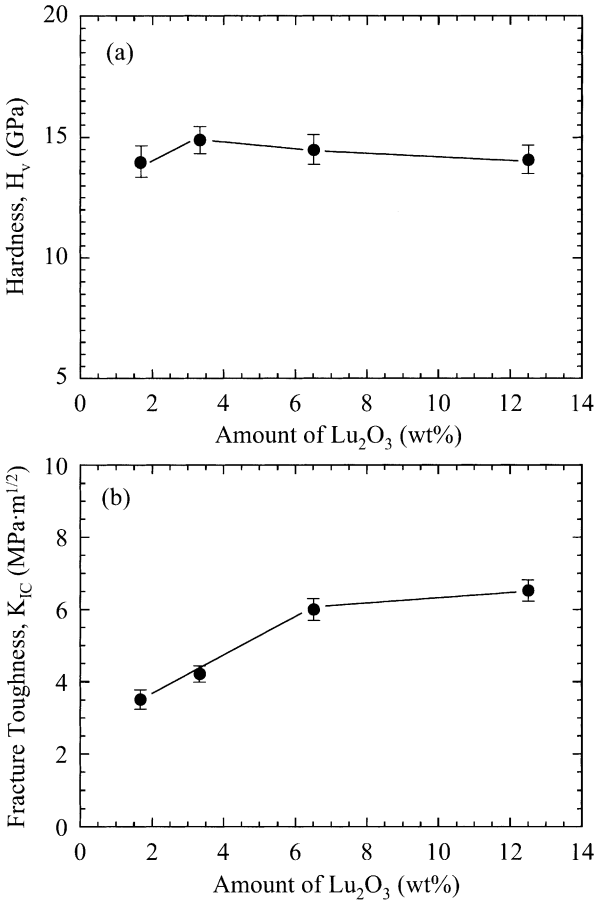


Fig. 6. (a) Hardness and (b) fracture toughness of the hot-pressed $Si_3N_4$ ceramics versus amount of $Lu_2O_3$ additives.

the evaluated hardness and fracture toughness tend to decrease with increasing indentation load (Table 3). The average hardness over all the indentation loads used was $H_v = 13.89$ GPa for 1.68 wt.% $Lu_2O_3$, $H_v = 14.90$ GPa for 3.33 wt.% $Lu_2O_3$, $H_v = 14.48$ GPa for 6.52 wt.% $Lu_2O_3$, $H_v = 14.08$ GPa for 12.51 wt.% $Lu_2O_3$. The corresponding average fracture toughness is $K_{IC} = 3.46$ MPa m$^{1/2}$ for 1.68 wt.% $Lu_2O_3$, $K_{IC} = 4.22$ MPa m$^{1/2}$ for 3.33 wt.% $Lu_2O_3$, $K_{IC} = 6.00$ MPa m$^{1/2}$ for 6.52 wt.% $Lu_2O_3$, $K_{IC} = 6.53$ MPa m$^{1/2}$ for 12.51 wt.% $Lu_2O_3$. These values are nearly the same as those reported on the hot-pressed $Si_3N_4$ ceramics with $Yb_2O_3$ and $Y_2O_3$ additives[3,4,15] except for the measured value at 1.68 wt.%, which is lower due to incomplete densification.

Table 3
Vickers indentation results of hot-pressed $Si_3N_4$ ceramics with $Lu_2O_3$ additives

| Amount of $Lu_2O_3$ (wt.%) | Load $P$ (N) | Diagonal $2a$ (μm) | Crack length $c$ (μm) | Hardness $H_v$ (GPa) | Fracture toughness $K_{IC}$ (MPa m$^{1/2}$) |
|---|---|---|---|---|---|
| 1.68 | 98 | 113.8±2.4 | 160.0±5.3 | 14.25±0.62 | 3.51±0.21 |
| | 196 | 161.4±3.3 | 264.8±15.3 | 13.97±0.58 | 3.48±0.25 |
| | 294 | 201.4±5.3 | 358.2±6.8 | 13.46±0.69 | 3.38±0.16 |
| 3.33 | 98 | 110.4±1.5 | 143.6±3.8 | 14.92±0.41 | 4.34±0.13 |
| | 196 | 156.6±2.6 | 236.4±5.6 | 14.83±0.49 | 4.12±0.14 |
| | 294 | 191.0±2.2 | 305.0±7.0 | 14.95±0.35 | 4.20±0.10 |
| 6.52 | 98 | 111.2±3.3 | 115.4±2.1 | 14.73±0.86 | 6.16±0.31 |
| | 196 | 159.6±2.7 | 189.2±5.0 | 14.28±0.49 | 5.82±0.27 |
| | 294 | 194.4±2.1 | 243.4±8.1 | 14.43±0.31 | 6.02±0.32 |
| 12.51 | 98 | 113.6±2.7 | 109.2±1.9 | 14.10±0.65 | 6.72±0.28 |
| | 196 | 160.0±2.7 | 177.8±5.3 | 14.21±0.48 | 6.48±0.28 |
| | 294 | 197.8±2.4 | 236.2±7.1 | 13.94±0.34 | 6.40±0.24 |

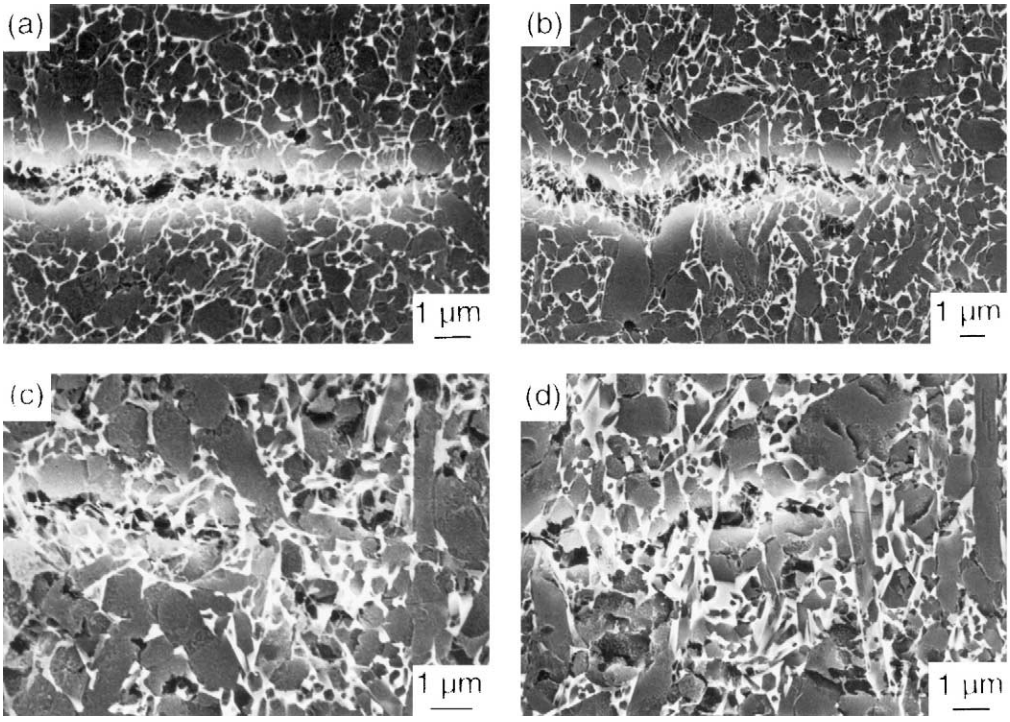


Fig. 7. Crack propagation behavior of the hot-pressed $Si_3N_4$ ceramics with $Lu_2O_3$ additives of (a) 1.68, (b) 3.33, (c) 6.52 and (d) 12.51 wt.%.

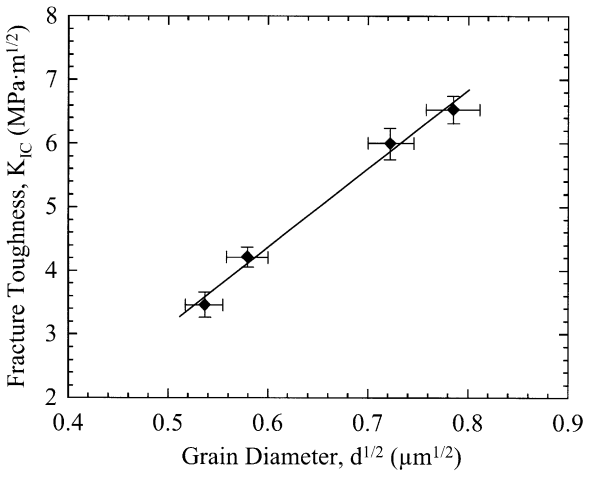


Fig. 8. Fracture toughness of the hot-pressed $Si_3N_4$ ceramics with $Lu_2O_3$ additives versus grain-section diameter, showing a dominated effect of grain diameter on fracture toughness.

The crack propagation behavior was studied using SEM imaging on Vickers indentation cracks in several plasma-etched samples, as shown in Fig. 7 . In the $Si_3N_4$ with 1.68 wt.% $Lu_2O_3$, the predominantly intergranular crack path is observed and there is little interaction between the crack and grains [Fig. 7(a)]. In addition, the thinner grain boundary phase, with a net-like shape, still remains connected, acting as elastic bridging over the crack faces. This phenomenon differs from $Si_3N_4$ with other kinds of additives and no similar behavior was seen.[4,6] This crack propagation characterization remains up to 3.33 wt.% $Lu_2O_3$ exception the grain boundary phase amount increases [Fig. 7(b)]. When the amount of additive increases to 6.52 wt.%, the crack tends to be deflected around larger grains [Fig. 7(c)], it is also seen to cut elongated grains. This suggests that it is energetically favorable for the crack to cut elongated grains, rather than be deflected by them or pull them out. Furthermore, a thicker and scattered grain boundary phase is observed instead of the thinner grain boundary phase. This indicated that an extensive interaction between the crack and the grains occurred, meaning the higher fracture toughness in the $Si_3N_4$ with 6.52 wt.% $Lu_2O_3$ than that in $<6.52$ wt.% $Lu_2O_3$. With further addition of $Lu_2O_3$, no noticeable change in the crack propagation behavior is observed exception for an increase in grain boundary phase amount [Fig. 7(d)].

The fracture toughness depends on the grain size, shape, volume fraction of the bridging grains, and frictional sliding stress between the grains.[4–6] A dependence of fracture toughness of $Si_3N_4$ on grain-section diameter is shown in Fig. 8 . An approximately linear relationship is seen between the fracture toughness and grain-section diameter, that is the bigger is the grain diameter and the higher is the fracture toughness. This suggests that the fracture toughness of $Si_3N_4$ is mainly dominated by the grain diameter; especially the elongated grains are effective for increasing fracture toughness.

## 4. Conclusions

Silicon nitride ceramic with various amounts of $Lu_2O_3$ additive was produced using the hot-pressing process. The elastic moduli were determined by means of ultrasonic measurements, and the fracture toughness was measured using Vickers indentation. The observed elastic moduli were higher than those of silicon nitride using other additives, and the measured fracture toughness was found to be comparable to that of these other materials. From these results, the following conclusions may be drawn:

1. The densification of silicon nitride by hot-press sintering was dependent on the amount of $Lu_2O_3$ additive and approximately 3.33 wt.% $Lu_2O_3$ was needed to densify $Si_3N_4$ completely at 1950 °C under a pressure of 20 MPa.
2. The hot-pressed silicon nitride with 1.68 wt.% $Lu_2O_3$ consisted of β-$Si_3N_4$ matrix with $Lu_4Si_2O_7N_2$ grain boundary phase, and this composition remained up to 6.52 wt.% $Lu_2O_3$, where as a new $Lu_2SiO_5$ phase was identified in the silicon nitride with 12.51 wt.% $Lu_2O_3$. The β-$Si_3N_4$ grain-section diameter was observed to increase with increasing amount of additive, and this increase was clearly noticeable as the amount of additive was equal to or greater than 6.52 wt.%.
3. The elastic moduli of the hot-pressed silicon nitride increased with an increase in amount of additive for incompletely dense material. However, the shear modulus and Young's modulus remained nearly constant independent of additive amount, and the bulk modulus slightly increased with amount of additive for completely dense material. The average values of the elastic moduli for completely dense $Si_3N_4$ were found to be: $G=132$ GPa, $E=338$ GPa, $B=255$ GPa and $\nu=0.28$.
4. The fracture toughness of the hot-pressed silicon nitride was found to increase rapidly with the amount of $Lu_2O_3$ up to 6.52 wt.%, and then to increase slowly. The grain-section diameter dominated the fracture toughness.

## References

1. Tsuge, A., Nishida, K. and Komatsu, M., Effect of crystallizing the grain-boundary glass phase on the high-temperature strength of hot-pressed $Si_3N_4$ Containing $Y_2O_3$. *J. Am. Ceram. Soc.*, 1975, **58**(7–8), 323–326.
2. Sanders, W. A. and Mieskowski, D. M., Strength and microstructure of intered $Si_3N_4$ with rare-earth-oxide additions. *Ceramic Bulletin*, 1985, **64**(2), 304–309.

3. Nishimura, T., Mitomo, M. and Suematsu, H., High temperature strength of silicon nitride ceramics with ytterbium silicon oxynitride. *J. Mater. Res.*, 1997, **12**(1), 203–209.
4. Park, H., Kim, H. E. and Niihara, K., Microstructure evolution and mechanical properties of $Si_3N_4$ with $Yb_2O_3$ as a sintering additive. *J. Am. Ceram. Soc.*, 1997, **80**(3), 750–756.
5. Mitomo, M. and Uesono, S., Microstructural development during gas-pressure sintering of α-silicon nitride. *J. Am. Ceram. Soc.*, 1992, **75**(1), 103–108.
6. Kleebe, H.-J., Pezzotti, G. and Ziegler, G., Microstructure and fracture toughness of $Si_3N_4$ ceramics: combined roles of grain morphology and secondary phase chemistry. *J. Am. Ceram. Soc.*, 1999, **82**(7), 1857–1867.
7. Yoon, K. J., Wiederthon, S. M. and Luecke, W. E., Comparison of tensile and compressive creep behavior in silicon nitride. *J. Am. Ceram. Soc.*, 2000, **83**(8), 2017–2022.
8. Park, H., Kim, H. W. and Kim, H. E., Oxidation and strength retention of monolithic $Si_3N_4$ and nanocomposite $Si_3N_4$-SiC with $Yb_2O_3$ as a sintering aid. *J. Am. Ceram. Soc.*, 1998, **81**(8), 2130–2134.
9. Nordberg, L. O., Nygren, M., Kall, P. O. and Shen, Z., Stability and oxidation properties of RE-α-sialon ceramics (RE = Y, Nd, Sm, Yb). *J. Am. Ceram. Soc.*, 1998, **81**(6), 1461–1470.
10. Moulson, A. J., Review reaction-bonded silicon nitride: its formation and properties. *J. Mater. Sci.*, 1979, **14**, 1017–1051.
11. Hirosaki, N., Yamamoto, Y., Nishimura T. and Mitomo, M. Japan Patent 324327, 2000.
12. Guo, S. Q., Hirosaki, N., Yamamoto, Y., Nishimura, T. and Mitomo, M., Improvement of high-temperature strength of hot-pressed sintering silicon nitride with $Lu_2O_3$ addition. *Scripta Materialia*, 2001, **45**(7), 867–874.
13. Guo, S. Q., Hirosaki, N., Yamamoto, Y., Nishimura, T., Mitomo, M., Strength retention in hot-pressed silicon nitride ceramics with $Lu_2O_3$ additives after oxidation exposure in air at 1500 °C. *J. Am. Ceram. Soc.*, in press.
14. Phani, K. K. and Nioygi, S. K., Elastic modulus-porosity relation in polycrystalline rare-earth oxides. *J. Am. Ceram. Soc.*, 1987, **70**(12), C-362-C-366.
15. Yeheskel, O. and Tevet, O., Elastic moduli of transparent yttria. *J. Am. Ceram. Soc.*, 1999, **82**(1), 136–144.
16. Anstis, G. R., Chantikul, P., Lawn, B. R. and Marshall, D. B., A critical evaluation of indentation techniques for measuring fracture toughness: I, direct crack measurements. *J. Am. Ceram. Soc.*, 1981, **64**(9), 533–538.
17. Yeheskel, O., Gefen, Y. and Talianker, M., Hot-isostatic pressing of $Si_3N_4$ with $Y_2O_3$ additions. *J. Mater. Sci.*, 1984, **19**, 745–752.
18. Guo, S. Q., Hirosaki, N., Yamamoto, Y., Nishimura, T., Kitami Y. and Mitomo, M. Microstructural characterization of hot-pressed silicon nitride ceramics with $Lu_2O_3$ additives. *J. Am. Ceram. Soc.*, submitted.